THESIS

WIND INDUCED STRESSES ON TREEHOUSE STRUCTURES

Submitted by

William E. Bradley

Department of Civil and Environmental Engineering

In partial fulfillment of the requirements

For the Degree of Master of Science

Colorado State University

Fort Collins, Colorado

Spring 2011

Master's Committee:

Advisor: Paul Heyliger

Marvin Criswell
Scott Glick

ABSTRACT

WIND INDUCED STRESSES ON TREEHOUSE STRUCTURES

Treehouses have recently become a profitable public attraction in the United States. With this increase in popularity, it becomes important to standardize treehouse engineering practices as an important step towards regulation of these structures.

This thesis outlines common practices among treehouse engineers and makes suggestions for calculation of the self-weight of a tree and stresses due to gravity and wind loads. In particular, this thesis uses a finite element model to analyze a foliage-free cottonwood tree with a rectangular treehouse under typical maximum wind loadings. Six scenarios are investigated, with a treehouse at different heights. Elastic analysis is used to determine the stresses due to wind near the base of the tree.

ACKNOWLEDGEMENT

First and foremost, I would like to thank my advisor Dr. Heyliger for his steady support and reassurance throughout the thesis composition process.

I would also like to thank Dr. Marvin Criswell and Dr. Scott Glick for being a part of my graduate academic committee.

DEDICATION

To Kara, for her loving support.

To Chad, who piqued and renewed my interest in this topic.

TABLE OF CONTENTS

1. INTRODUCTION 1

2. LITERATURE REVIEW 4

2.1 INTRODUCTION 4

2.2 TREE STEM MECHANICS AND ANALYSIS 4

2.2.1 Living wood as a structural material 4

2.2.2 Modeling a tree as a column in a structure 6

2.2.3 Failure modes of the tree stem 7

2.2.4 Multiple stem installations and torsion 8

2.3 ROOTS AND FOUNDATION 9

2.3.1 Roots modeled as a fixed end 9

2.3.2 Failure modes of the roots 12

2.4 ANCHORAGES BETWEEN TREE AND TREEHOUSE 13

2.4.1 The Garnier limb 13

2.4.2 Arrestor bracket 13

2.5 DEFLECTION, VIBRATIONS, AND OTHER SERVICEABILITY ISSUES 13

2.6 TREE GROWTH AND OTHER BIOMECHANICAL CONCERNS 14

2.6.1 Age and life span 14

2.6.2 Disease, decay, and wood-eating insects 15

2.6.3 Stress response 16

3. TREE MODELED AS A LINEARLY TAPERED COLUMN 18

3.1 TREE CIRCUMFERENCE VS. HEIGHT: A SIMPLE EXPERIMENT 18

4. STRESSES FROM WIND LOADS: RESULTS AND DISCUSSION 21

4.1 GENERAL STRUCTURAL ANALYSIS PROCEDURES 21

4.1.1 Design loads 21

4.2 FINITE ELEMENT ANALYSIS OF A TREE-TREEHOUSE SYSTEM UNDER WIND LOADS 29

4.2.1 Elastic analysis principles and tree geometry 29

4.2.2 The finite element method for a 1-D beam (direct stiffness method) 32

4.2.3 Using the 1-D beam code to calculate stresses and deflections 33

5. DISCUSSION OF EXISTING CHALLENGES 38

5.1 REGULATION OF TREEHOUSE STRUCTURES 38

5.2 MATERIAL STRENGTHS FOR DIFFERENT TYPES OF LIVING WOOD 39

5.3 THE DIFFICULTY OF GEOMETRY IN TREEHOUSE ENGINEERING 40

5.4 BUCKLING AND SECOND ORDER EFFECTS 41

5.5 SECONDARY EFFECTS OF RAIN, SNOW, AND ICE 42

6. CONCLUSIONS 43

7. WORKS CITED 45

APPENDIX 1: STUTTGART TABLE OF WOOD STRENGTH (PARTIALLY REPRODUCED FROM (BRUDI & VAN WASSENAER, 2001) 51

APPENDIX 2: RESULTS OF TREE CIRCUMFERENCE VS. HEIGHT 53

APPENDIX 3: PROJECTED AREA OF A PRISTINE (BINARY) TREE SILHOUETTE 54

APPENDIX 4. BEAM.M (MATLAB CODE) 58

LIST OF FIGURES

Figure 1. Tapered cantilever beam-column 7

Figure 2. The tensile fork. Reprinted from (Mattheck C. , 1991, p. 37). 9

Figure 3. Mechanical features governing root anchorage stability of a stereotypical Pachycereus pringlei plant with stem height h and bayonetlike root depth L. Reprinted from (Niklas, 2001, p. 17). 11

Figure 4. Root flare shown as having a dramatic taper 19

Figure 5. Negative silhouette of tree 2 23

Figure 6. Silhouette partition from 30-40 feet with superimposed rectangular treehouse 25

Figure 7. Silhouette area vs. treehouse height 26

Figure 8. Exposure coefficients for height ranges 27

Figure 9. Tree as a finite element beam 31

Figure 10. Critical stresses near base of tree due to wind loads 34

Figure 11. Allowable compressive load vs. treehouse installation height 35

Figure 12. Tree circumference vs. height for six trees 53

Figure 13. Binary silhouette of a tree..... 54

Figure 14. Binary silhouette, 201-600 pxl 55

Figure 15. Binary silhouette, 601-1000 pxl 55

Figure 16. Projected area vs. height of a pristine silhouette 56

1. INTRODUCTION

The view is often taken that treehouses are a subsidiary residential structure; a novelty, designed and built by their future occupant, purely for the purpose of enjoyment. Indeed, treehouses are eye-catchers, garnering aesthetic appeal, a direct connection with nature, and a lofty view of surrounding vistas. They also have an incredible ability to capture the imagination and remind us of what it feels like to be a kid. Current commercial treehouse resorts offer most of the same amenities of a hotel, including in-room toilet, shower, and electricity (Greenwood & Garnier, Habitable Treehouses: Not as Simple as Swiss Family Robinson). It is for these reasons and others that treehouses have been featured in magazines like Forbes Life, as some treehouses go beyond backyard projects to gain attention in the United States and Europe as commercially viable vacation destinations (Hochman, 2010).

Treehouses and tree-supported structures have been used for public functions in Europe for centuries. The Dancing Lime Treehouse in Peesten, Germany, was built circa 1760 and still serves as a platform for public functions (Nelson, 2004). The great oak tree Chêne chapelle in Seine-Maritime, Normandy, France, houses two chapels: *Notre Dame de la Paix* and *Chambre de l'Ermite*, both built in 1669 (Atlas Obscura, 2011). Also built in the seventeenth century is the Pitchford Hall in Shropshire, England, which is the oldest treehouse still in existence (Henderson & Mornement, 2005). These

structures represent only a small part of the rich history and ongoing public interest with treehouses.

While these structures have been available for community use for hundreds of years in Europe, it was not until 1998 that a treehouse was first made to follow code for public use in the United States (Garnier, LegaliTrees). There are now over a dozen engineering firms in the United States that provide the service of custom treehouse design and construction for private and public use (Fulton, Professional tree house building companies, 2010).

With treehouses increasing in popularity in the public sector, a need arises to find a way to regulate these structures and to find reliable methods to determine their capacity and factor of safety. In the design of traditional structures, civil engineers are expected to apply their knowledge of structural analysis and mechanics to follow government-approved building codes. It is a rare case when such a specific provision for treehouses is included in local building doctrines.

Even if specified regulations were more common, determining the safety of a tree-supported structure is a process with many unknowns. For each project, the engineer is required to design and analyze a structure that is built on a unique, organic, and unpredictable foundation and column: the roots and trunk of the supporting tree. Unlike cut timber, trees have twists and bends, inconsistencies in their tissue, and cannot be sized, making internal stresses and strengths difficult to determine. Unlike a cast-in-place foundation with known physical properties, the root structure of a tree is complex and grown almost entirely underground, making its volume and overall efficacy difficult to

assess. In addition, wind loads on a tree are difficult to determine because the surface area projections of the trunk, branches, and leaves are a challenge to calculate exactly. Tree branches and stems also grow with age, and so design provisions must be made to the treehouse to allow for this. A final variable is that trees are susceptible to disease, decay, and death, all of which can severely compromise their ability to resist load.

As with other fields of engineering, current design practices in the field of treehouse engineering have the purpose of circumventing the intricate evaluations and calculations that would be necessary for exact analysis. Most of the time, approved empirical formulas and even the finite element method are considered acceptable replacements, though direct testing of the critical components of a tree may still be necessary on a case-by-case basis.

This thesis highlights some of the current practices and concerns involved in treehouse engineering and looks at the major mechanical issues involved with a single-tree installation of a treehouse. In particular, this thesis highlights the major structural aspects of a tree in its ability to support itself and an attached treehouse under typical wind and gravity loadings. It looks at the mechanics of a tree stem as a compressive member, also subject to bending, modeling the tree trunk as a tapered beam-column and the function of the roots as a fixed foundation.

Specifically, a finite element analysis is used to calculate the effects of wind loads acting on the entire tree on flexural compressive stress acting near the base of the tree. The projected area of a treehouse is assumed at five different heights. Lateral deflections and allowable gravity loads are calculated through this method.

2. LITERATURE REVIEW

2.1 Introduction

An extensive literature search and consultation with treehouse engineer Charles Greenwood, P.E., has all but confirmed that no scholarly research articles in the public domain directly relate to structural engineering design in treehouses. This section reviews the aspects of tree mechanics and strength that are relevant to the topic at hand, and relates treehouse information from current building guides to provide an overview of current practices in the field.

2.2 Tree stem mechanics and analysis

To understand the way a treehouse is able to transfer loads to the ground, it is fundamental to understand the mechanics of a tree and how a structural engineer might model this complex organism as a structural member.

2.2.1 Living wood as a structural material

Living wood can be approximated as an elastic, orthotropic material (Bodig & Jayne, 1993). Its fibers follow the direction parallel to its grain from the roots of the tree up the stem through the branches (Mattheck C. , 1991). In agreement with these premises, the American Forest & Paper Association and the American Wood Council, in the National Design Specification® for Wood Construction (NDS), suggest the use of basic elastic analysis to determine flexural stresses in wood (American Forest & Paper

Association, American Wood Council, 2006). This type of analysis involves the use of fundamental mechanics equations to calculate the stresses a structural member is expected to endure for a given transient or a long loading time. It then compares these stresses with the minimum strength of the material expected to carry the load. Elastic analysis is used to calculate bending stresses in Section 4.

The strengths of living wood vary widely from species to species, and also depend on other factors such as wood density, knots and local grain deviations, decay, and hollowness (Mattheck, Betge, & West, Breakage of hollow tree stems, 1994). There is also a difference in strength of living wood within each tree. Heartwood and sapwood differ in strength. Also, wood differs in density and strength, increasing from top to bottom.

Brudi & van Wassenaer (2001) concede that data on living wood is not widely available. The authors explain that this is partly because the forestry industry and other entities with the resources necessary to conduct stress tests have little interest in finding these values. The properties of living wood are often overlooked because dried, cut wood is the material used to make most every product in the industry.

These authors decide to use data found by Wessolly and Erb (Brudi & van Wassenaer, 2001). In order to study green, living wood strength, Wessolly and his team conducted tests in the lab and compiled a table that includes strength, stiffness, and aerodynamic drag data of several species of European and American trees. This table, called the *Stuttgart table of wood strength*, is partially reproduced and adapted in Appendix 1 to include United States customary units and common names for each

species. A useful addition to this table would be the inclusion of the modulus of rupture, tension parallel to the grain, and shear perpendicular to the grain for each wood species listed, as have been included in the NDS (American Forest & Paper Association, American Wood Council, 2006).

Comparing the available reference design values for select species found both in the NDS and in the Stuttgart reference reveals the general trend that living wood tends to have more raw compressive strength, but also tends to be slightly less stiff than timber. This is an expected trend due to the higher moisture content in living wood. However, there are many design value adjustment factors in NDS than must be considered for a more precise analysis (American Forest & Paper Association, American Wood Council, 2006).

2.2.2 Modeling a tree as a column in a structure

To simplify calculations and to keep the scope of this project reasonable, analysis is specific to a single tree installation. From the ground up, the roots of the tree represent the foundation, which effectively clamps the tree's stem, or trunk. The trunk can then be visualized as a tapered vertical cantilever beam-column that bears the gravity loading of the remaining stem, branches, and leaves and supports any lateral loading (Mattheck C. , 1991). Below is an illustration of this type of model:

Figure 1. Tapered cantilever beam-column

This figure shows that the tree stem modeled as a round, tapered cantilever beam-column with a mass, *m*, loaded at its end. Let the mass represent the loads to be carried by the trunk of the tree to its roots. This mass includes the remaining stem, branches, and the addition of a structure. The tree transmits loads to its roots directly through axial compression and lateral loads through bending moments; modeled as above, the tree resists combined loading types (Niklas, 2001).

2.2.3 Failure modes of the tree stem

2.2.3.1 Rupture

For dried timber and lumber, the NDS (2006) gives reference values for modulus of rupture for many species of wood. These represent the nominal strength each species and grade has when it undergoes pure bending. A value for strength implies capacity before failure is likely, and therefore represents a mode in which the wood of a tree can fail. However, until an explicit relationship between NDS reference values for dry wood and living tree strength can be determined, these values do not directly relate to those that would be found in the field.

2.2.3.2 Compression

Compression strengths were found by Wessolly and Erb for numerous species as described above and presented in Appendix 1 (Brudi & van Wassenaer, 2001). There is therefore direct reference of compression strength as a failure mode, as cross-sections of trees were compressed to failure in the lab before any change in moisture could occur.

2.2.3.3 Buckling

Mattheck (1991), in his book Trees: The Mechanical Design, mentions that no tree has ever been observed to have buckled under its own weight.

2.2.4 Multiple stem installations and torsion

Though it is beyond the scope of this thesis, treehouses can be built on multiple trees or multiple stems of the same tree. In fact, this is the most common way for these structures to be installed, especially if they are appreciable in size. This approach can have an overall beneficial result, as it can reduce the axial load and flexural moment felt by each stem. This allows larger structures to be built with an assumed higher factor of safety (Greenwood C. , 2010).

On the other hand, there are complications that result as well. Differential deflections between trees in the same system can cause tensile, compressive, and shearing forces on the structure. Also, lateral deflection can cause an increase in torsion. To reduce this torsion, the development of the regulation of a type of decoupling mechanism is desired (Greenwood C. , 2010).

For a single tree with multiple stems, Mattheck (1991) presents a case study in which he highlights an area of higher tension located on the interior bifurcation point between the stems. The addition of a structure would increase this type of stress.

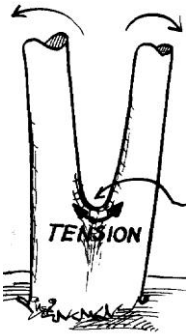

Figure 2. The tensile fork. Reprinted from (Mattheck C. , 1991, p. 37).

Following the drawing above, Mattheck (1991) is clear to indicate that trees grow extra wood at bifurcation points to combat increases in tension at these locations.

To prevent splitting or adding to this tension at the bifurcation point, Nelson and Hadden (1997) suggest the use of a cable to tie the stems together. This procedure allows the cable to take most of the excess tensile force instead of the tree. The author does not explain the effects of tree growth in this case.

2.3 Roots and foundation

2.3.1 Roots modeled as a fixed end

Like the fixed end of a cantilevered beam or column, the roots of a tree must ultimately resist all forces and moments applied to the tree through their connection with the earth in order for equilibrium to be achieved. Roots vary widely in shape and thus in the way this task is accomplished. The three force-type motions resisted in a cantilever

beam-column loaded in this manner are vertical compression, horizontal shearing, and moment, with the latter most commonly controlling (Leet, Uang, & Gilbert, 2008).

2.3.1.1 Vertical compression

It is common knowledge that the Earth must ultimately resist all vertical loads, and it is assumed that the roots are able to distribute and diffuse the vertical load of the tree very well due to their relatively large surface area when compared to the stem. Root bearing capacity is not discussed in this thesis.

2.3.1.2 Shear

No scholarly articles detailing shear behavior in trees were found, and shear is not described as a mode of failure in any scholarly works researched. However, the NDS (2006) does detail design for shear in all bending members. For this reason, shear should be examined for trees if experimental values can be found for the shear strength of living tissue.

2.3.1.3 Moment resistance

There are two ways that roots interact with the soil to resist movement: normal pressure and claying friction. Niklas (2001) presents the idea that "bayonetlike" roots are able to resist moment because their penetration into the ground allows the soil to enact lateral earth pressures on them. These pressure distributions act opposite each other about a pivot point, which can be analyzed as a point moment at that location that resists the moment created from loading. The pivot point is located approximately at the surface when lateral root restraints are present and at mid-span of the root depth when they are not:

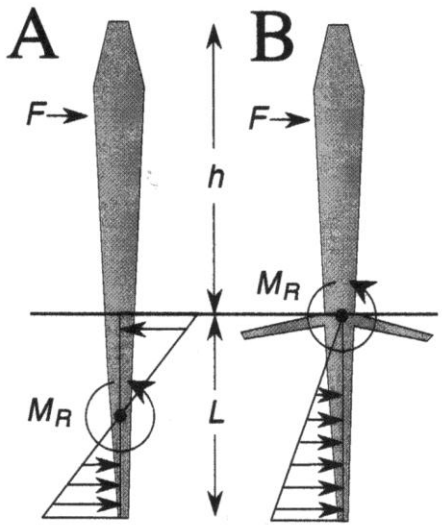

Figure 3. Mechanical features governing root anchorage stability of a stereotypical Pachycereus pringlei plant with stem height h and bayonetlike root depth L. Reprinted from (Niklas, 2001, p. 17).

This diagram shows the general way a tap root structure provides resistance to moment due to applied lateral forces high on its stem by direct lateral earth pressures.

Greenwood (2010) states that the roots also resist moment through "claying friction", which implies that the large amount of surface area the roots provide is able to resist motion by friction. This argument implies that earth pressures acting normal to the root surface help to enforce shear traction between the roots and the soil.

Lateral earth pressures and claying friction are both ways the earth prevents the roots of a tree from moving in a horizontal direction. This ability is granted as a function of the characteristics of the soil particles and the way in which they interact with the roots and with themselves. Soil tests can be conducted to determine soil properties such as specific weight, saturation, and frictional factors. However, it remains difficult to find the area and spatial arrangement of a given underground root structure, and thereby

precisely calculate the tree's ability to resist moment at its base. Considering then a proposed treehouse, it becomes desirable to conduct empirical tests that would represent the proposed lateral loads at the structure's mounting location.

An example of this type of test involves placing a strap, equipped with a force gauge, a short distance above the base of the tree and pulling with a force that would represent the overturning moment caused by lateral loads on the tree and treehouse (Nelson & Hadden, 1997).

2.3.2 Failure modes of the roots

Two failure modes for the roots of a tree were found: uprooting and root delamination. Both failure modes result in the roots' inability to resist moment. While delamination of the roots infers failure of the roots themselves, uprooting usually occurs as a result of the roots growing in soil that cannot handle the overturning moment caused by lateral loads on the tree.

2.3.1.1 Uprooting

Illustrations in Das (2006) suggest that uprooting failure may be similar to tension failure in shallow foundations. Details are not discussed.

2.3.1.2 Root delamination

In this type of failure, the outer layer of the roots is stripped from the inner layer, failing in shear at the interface. Again, illustrations in Das (2006) suggest that this type of failure may be similar to tensile failure in foundation piles.

2.4 Anchorages between tree and treehouse

There are several connections that can be used to attach a structure to a tree. Two of the methods described by designers are discussed below.

2.4.1 The Garnier limb

Nelson (2004) refers to the Garnier Limb, "GL", or otherwise called a lag bolt, as a treehouse technology breakthrough. Developed by Greenwood, the bolt is a human-made, turn-steeled limb, with a collar attached above the threads. The Garnier Limb, capable of carrying an excess of 9,000 pounds to the tree stem, is used in the common scenario where load needs to be carried in the absence of an actual tree limb. The design of this hardware has been tested by Greenwood (2010), and has been modified many times over the years.

2.4.2 Arrestor bracket

The arrestor bracket is a rectangular connector that encompasses the "GL". Main support beams are bolted to the arrestor bracket, which in turn transfers load to the "GL".

2.5 Deflection, vibrations, and other serviceability issues

A prominent performance issue in treehouses is the possibility of large lateral deflections due to wind loads. This is particularly noticeable during the first year after installation of a treehouse, when the tree has not adapted yet to the increased gravity loadings (Greenwood C. , 2010). Deflections due to wind loads are investigated in Section 4.

2.6 Tree growth and other biomechanical concerns

The tree or group of trees, in essence, dictates the practical size, orientation, type, and maximum loading of a treehouse. Therefore, a proper inspection into each tree's age, growth, and general health is an integral part of selecting a treehouse site. This step is so important, in fact, that the expert assessment by an arborist or tree surgeon is usually required to gain confidence in the safety of the tree used for a treehouse installation (Nelson & Hadden, 1997).

In addition, the tree continues to grow after a treehouse is built. The rate of growth is species dependent. This section also looks at the ways a tree responds to added stress over time.

2.6.1 Age and life span

Age is an important factor when selecting a tree as a site for a treehouse. The tree must be mature, such that it will have a large cross-section to resist load. It also must have limited potential for further growth, so that the tree does not expand in a way that it pushes on the structure. To allow for growth of even a mature tree, Nelson (2004) recommends that two inches be left between the tree trunk surface and the treehouse structure.

The age and life span of trees varies greatly, and some trees do not live for much more than fifty years. However, many trees live for well over one hundred years (Jacobson, 2001). A commonly-held belief is that it is good engineering practice to design a structure that will last for fifty years. With both of these ideas in mind, it is quite reasonable to infer that a treehouse could be built in the right tree to last for

decades. The only caveat is that construction takes place after a tree reaches full maturity, which is the practice of treehouse designers Wenning (2009), Fulton (2007), Nelson and Hadden (1997), and Greenwood (Greenwood & Garnier).

After selecting a likely building site, authors Wenning (2009), Nelson, and Hadden (1997) recommend seeking the expertise of an arborist who would be able to surmise the age, health, and life expectancy of the tree. This should be done before any structural planning is initiated.

2.6.2 Disease, decay, and wood-eating insects

When selecting a tree for a treehouse, an engineer's first concern should be the health of the tree. A tree that has been exposed to disease, decay, or wood-eating insects has been compromised in its structural integrity, and should not be selected as a support for a treehouse (Nelson & Hadden, 1997). Designers Wenning (2009), Fulton (2007), Nelson and Hadden (Nelson & Hadden, 1997) agree on this, and all have contributed layman tests to determine if a tree's health has been compromised in some way. Both Wenning (2009) and Nelson & Hadden (1997) mention looking for missing or dead sections of the crown and assessing the quality and intactness of the bark at the root flare. The latter is done by creating small, shallow scuffs about the perimeter of the tree and checking for decay or discoloration. Healthy colors include pink, red, and green (Nelson & Hadden, 1997).

With respect to decay, Wenning (2009) lists "the formation of cracks all the way through the edge, exposed decay (wood largely decomposed, outer wall of the trunk partially disintegrated), growth deficits, supply bottlenecks (bark and cambium dying

off), noticeable grooves in the trunk..." (p 35) as indicators of decay of the stem. In addition, he also adds that ultrasound tomography can be used to determine the quality of the wood of an entire cross-section, and does not require drilling. However, even if no signs of tree illness can be easily diagnosed, Wenning (2009) recommends professional consultation from an arborist or tree surgeon is always the safest route.

Disease and decay can both be made more probable when a tree has endured excessive damage to its bark or cambium layer. It is for this reason and others that designers have instructed to build in a manner that does the least amount of damage possible (Fulton, Build your own treehouse, 2007).

2.6.3 Stress response

A major asset to trees' survival is their ability to adapt to changes in their physical surroundings. In particular, their ability to conform to changes in gravity and wind loads is of the most importance in regards to the design of a treehouse (Niklas, 2001). To cope with changes in stress, trees have receptors that detect those changes, and with time are able to reinforce the most critical regions with more tissue.

Just as an engineer designing a wood beam might increase depth to accommodate an increased proposed loading, trees have their own way of bolstering themselves in situ. Studies have shown that trees will grow tissue of increased volume and density in regions where they experience elevated stress (Mattheck C. , 1991). In particular, empirical testing by Greenwood, showed that trees subjected to the increased loading of a treehouse are able to grow relatively strong tissue in locations of highest stress (Greenwood C., 2010).

This natural process effectively redistributes stress homogeneously to all fibers, thereby increasing strength capacity and stiffness (Mattheck C. , 1991). This effect happens in the roots as well, which change their geometry proportionally to the stresses they must handle (Niklas, 2001).

3. TREE MODELED AS A LINEARLY TAPERED COLUMN

3.1 Tree circumference vs. height: a simple experiment

It is unclear how to model the taper of a tree. Trees are not perfectly cylindrical with a uniform rate of change of diameter. There are knots, lower branches, bumps, twists, and many other abnormalities a tree can possess. Despite these deviations, the ability to approximate a linear taper would ease calculation, and allow for the analysis performed in Section 4 to be compared with calculations taken from NDS code provisions.

In order to estimate the rate of change in radius with height, several local cottonwood trees at Warren Park in Fort Collins were measured. The trees were chosen for their proximity and convenience. The purpose was to compare the change in circumference, and thus radius, with height to a linear distribution.

Upon inspection of each tree, it was immediately apparent that the there was a change in the taper above and below the root flare of the tree, as shown in Figure 4 below:

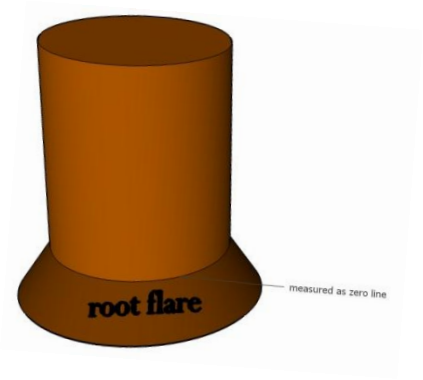

Figure 4. Root flare shown as having a dramatic taper

For the purposes of this study, the trees' circumferences were measured just above the highest root flare. The first six feet above this point of six different trees were measured. Six feet was the point below where the branches started to grow for most of the trees. The results of these measurements are listed in Appendix 2.

The collected data reveals a trend that a linear taper is approximate. R^2 values for linear fit ranged from 0.622 for Tree 1 to 0.958 for Tree 5. Tree 1 showed little to no change in circumference after the first two feet, indicating little to no taper.

The slope of the best fit line for each tree is the average change in circumference of that tree with height for the first 6 feet of the tree. Tree 2 was used for the analysis below and in Section 4. The change in radius for this tree is then given by:

$$r'(z) = \frac{C'(z)}{2\pi}$$

where $C'(z)$ is the slope of the best fit line for the circumference as a function of the height, z. For tree 2:

$$C'(z) = -2.1422\ \frac{in.}{ft}$$

$$\rightarrow r'(z) = \frac{C'(z)}{2\pi} = -0.341\frac{in}{ft}$$

where $r'(z)$ is the change in radius in inches per foot of height. This value cannot be used to extrapolate a circumference at locations significantly higher than the height region sampled. As will be explained below, the height of this tree, tree 2, was determined to be 61.3 feet. At this height, the radius of the tree in inches, defined as a linear function of the height z, in feet, becomes

$$r(z) = -0.341(z - 2) + 97$$

The radius becomes negative at 61.3 feet. Therefore, this experiment suggests that more samples must be taken in order to get an acceptable linear slope for the change in radius of a tree. Even then, a linear taper from top to bottom cannot be assumed.

4. STRESSES FROM WIND LOADS: RESULTS AND DISCUSSION

4.1 General structural analysis procedures

4.1.1 Design loads

Design loads must be established or approximated as a first step in order for a strength analysis to be possible. NDS (American Forest & Paper Association, American Wood Council, 2006) specifies six different types of loads: Dead, Live, Wind, Rain, Snow, and Earthquake.

The conglomerate sum of allowable gravity-type loads, including dead, live, rain, and snow loads was found from this analysis. Wind loads were examined in detail.

4.1.1.1 Gravity loads

In order to determine the overwhelming majority of dead load carried by a tree, it is necessary to approximate the volume and self-weight of the tree. These properties were not determined. Possible methods on how this could be achieved are discussed in the Discussion section of this thesis. Dead and live loads transmitted to the tree through the added treehouse are assumed to be small in comparison to the many thousands of pounds that make up the self-weight of the tree.

4.1.1.1.1 Line of loads

The line of loads for gravity in a treehouse is expected to travel from the floor of the treehouse, to its floor joists, and to its main support beams, which are bolted to the tree. The tree has its own line of loads, which is the branches or Garnier Limbs, to the stem, and to the roots.

4.1.1.2 Earthquake Loads

The effects of the earthquake loading were not studied, and are not expected to be controlling in the factored loads in the State of Colorado.

4.1.1.3 Wind Loads

These loads were modeled in sections as uniformly distributed loads, acting perpendicular to the stem of the tree, and varying in magnitude with height. The values of these loads were determined for Tree 2 using a silhouetting procedure similar to that discussed in Appendix 3.

Niklas (2001) uses a method of silhouettes to determine wind loads in trees. The projected area of the tree is found by examining its silhouette. This same method is used in the report *Area and volume measurements of objects with irregular shapes using multiple silhouettes* by Lee, Xu, Eifert, and Zhan (2006) to measure the projected area of plants. In both reports, details on how these exact areas were found are omitted. In general, small branches, twigs, and leaves bend greatly in the wind, thereby reducing the amount of drag they would otherwise cause, and reducing their surface area (Niklas, 2001). Therefore, using the projected area with leaves is assumed to be a conservative approach to calculating wind loads.

Both authors give the resultant wind force as:

$$W = p_w \cdot A_s$$

where p_w is a known wind pressure, and A_s is the area of the silhouette. In his analysis, Niklas (2001) uses the entire area of the tree, which does not include height effects and is inconsistent with structural analysis concepts detailed by Leet, Uang, and Gilbert (2008). This thesis uses height effects, and therefore represents a more accurate depiction of wind loads.

4.1.1.2.1 Determining the projected area of a cottonwood tree from Warren Park

As a preliminary step, the actual height of the tree was estimated through relative comparison of the lengths of shadows cast by sunlight at the same time of day. The shadows of an object of a known height and the tree were compared, and a proportion was used to find the estimated height of the tree as $61.3\ ft$.

Then, as discussed in the process detailed by Appendix 3, a silhouette of the tree was photographed:

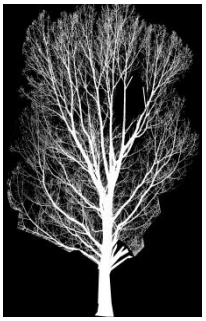

Figure 5. Negative silhouette of tree 2

The photograph was found to have a height of $2367\ pixels$. This was used to find a scaling factor of $\frac{2367pxl}{61.3ft} = 38.61\frac{pxl}{ft}$ between tree height in feet and photograph height in pixels. The scaling factor was then used to find the pixel heights needed to partition the photograph.

The picture was first altered to bring out contrast between the tree and the background. The negative was used for more immediate recognition of inconsistencies. The photo was partitioned into ten sections, which either relate to the twelve elements used in the following finite element analysis or to discretized exposure factors for wind loads as tabulated by Leet, Uang, and Gilbert (2008).

The area of white pixels was calculated using ImageJ, as described in Appendix 3. The corresponding projected area of the real tree was then found using the scaling factor, squared. The results produced are detailed in Table 1 below:

Table 1. Results of Area Calculations for Silhouette of Tree from Warren Park

Height Range (ft)	**Avg. Height (ft.)**	**Area of Silhouette (pxl)**	**Silhouette Area (ft^2)**
0-1.24	0.622	5390	3.615
1.24-10	5.622	32199	21.60
10-15	12.5	50793	34.07
15-20	17.5	71149	47.72
20-25	22.5	76881	51.56
25-30	27.5	85765	57.52
30-40	35	174689	117.1
40-50	45	138648	92.99
50-60	55	141455	94.87
60-61.3	60.65	4674	3.135

These results show the area of the tree at different height ranges. The height range of 0-1.24ft represents the height of the root flare, where the stem is tapered more

dramatically. The other height ranges were selected to match discretized exposure factors, as discussed below.

After successfully gathering data about the projected area of the tree, the image was altered. A white, twenty foot wide by ten foot high rectangle, representing the profile of a treehouse of these dimensions, was superimposed over the tree at five different heights: 10, 20, 30, 40, and 50 feet above the ground. The figure below shows what one altered silhouette partition might look like:

Figure 6. Silhouette partition from 30-40 feet with superimposed rectangular treehouse

The silhouette above approximates how a rectangular treehouse might appear as a silhouette. Each silhouette partition like the one above represents the combined projected area of a tree and treehouse. Anchorages and other practical concerns are ignored.

ImageJ and the scaling factor were again used to calculate new projected areas of the altered silhouettes. The non-dimensionalized results are charted below:

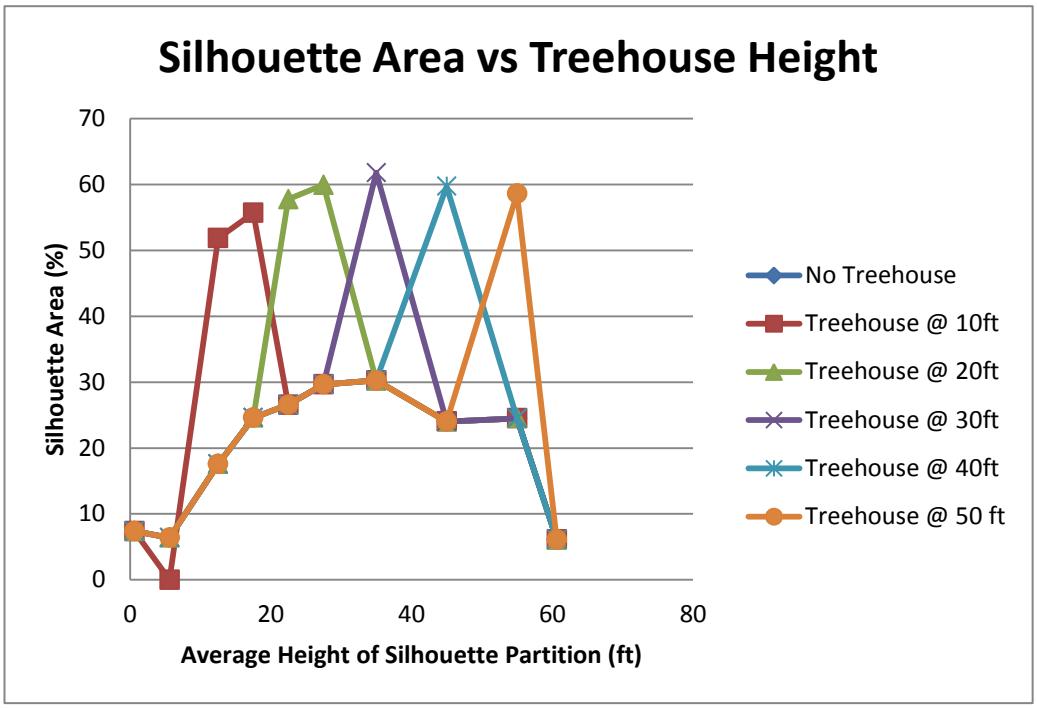

Figure 7. Silhouette area vs. treehouse height

This figure shows that the superimposed area of the treehouse drastically affects the projected area of the silhouette partitions at height domains in which it is installed. Upon inspection, a near constant jump in projected surface area at the treehouse location can be surmised.

4.1.1.2.2 Finding wind loads from projected areas

Once the projected areas were calculated, the data were used to find wind loads. Leet, Uang, and Gilbert (2008) state that wind loads should be calculated at each floor of a building. There are other factors that must be considered when calculating wind loads for a building, such as the importance of the structure, the exposure to wind, topography, wind directionality, gust factors, and others. The factored wind pressure is then given by:

$$q_z = 0.00256V^2IK_zK_{zt}K_d$$

where V is the basic wind speed for a region, I is the importance factor of the structure, K_z is the velocity pressure exposure coefficient, K_{zt} is the topographic factor, and K_d is the wind directionality factor. V was taken to be $100\ mph$, and I and K_{zt} as unity. The tree-treehouse system was considered to be round, specifying K_d as 0.95. The exposure factor, or coefficient K_z, is specified by a wooded area with low exposure, and varies with height. Values used for K_z are tabulated below:

Height Range (ft)	Avg. Height (ft.)	Exposure Coefficient
0-1.24	0.622	0.57
1.24-10	5.622	0.57
10-15	12.5	0.57
15-20	17.5	0.62
20-25	22.5	0.66
25-30	27.5	0.7
30-40	35	0.76
40-50	45	0.81
50-60	55	0.85
60-61.3	60.65	0.89

Figure 8. Exposure coefficients for height ranges

These coefficients made it possible for wind resultants to be calculated for each silhouette partition. It was desired to find an average, equivalent, and uniformly distributed load for each height range, which would later be used in finite element analysis for a one-dimensional beam. For each partition, the uniformly distributed load was calculated as:

$$w_p = \frac{q_z A_s}{h_p}$$

where A_s is the area of the silhouette for the partition and h_p is the height of that partition. The heights of the partitions would later be in agreement with the lengths of the corresponding elements of the beam used for finite element analysis. The uniformly distributed loads for each height of installation of the treehouse are charted below:

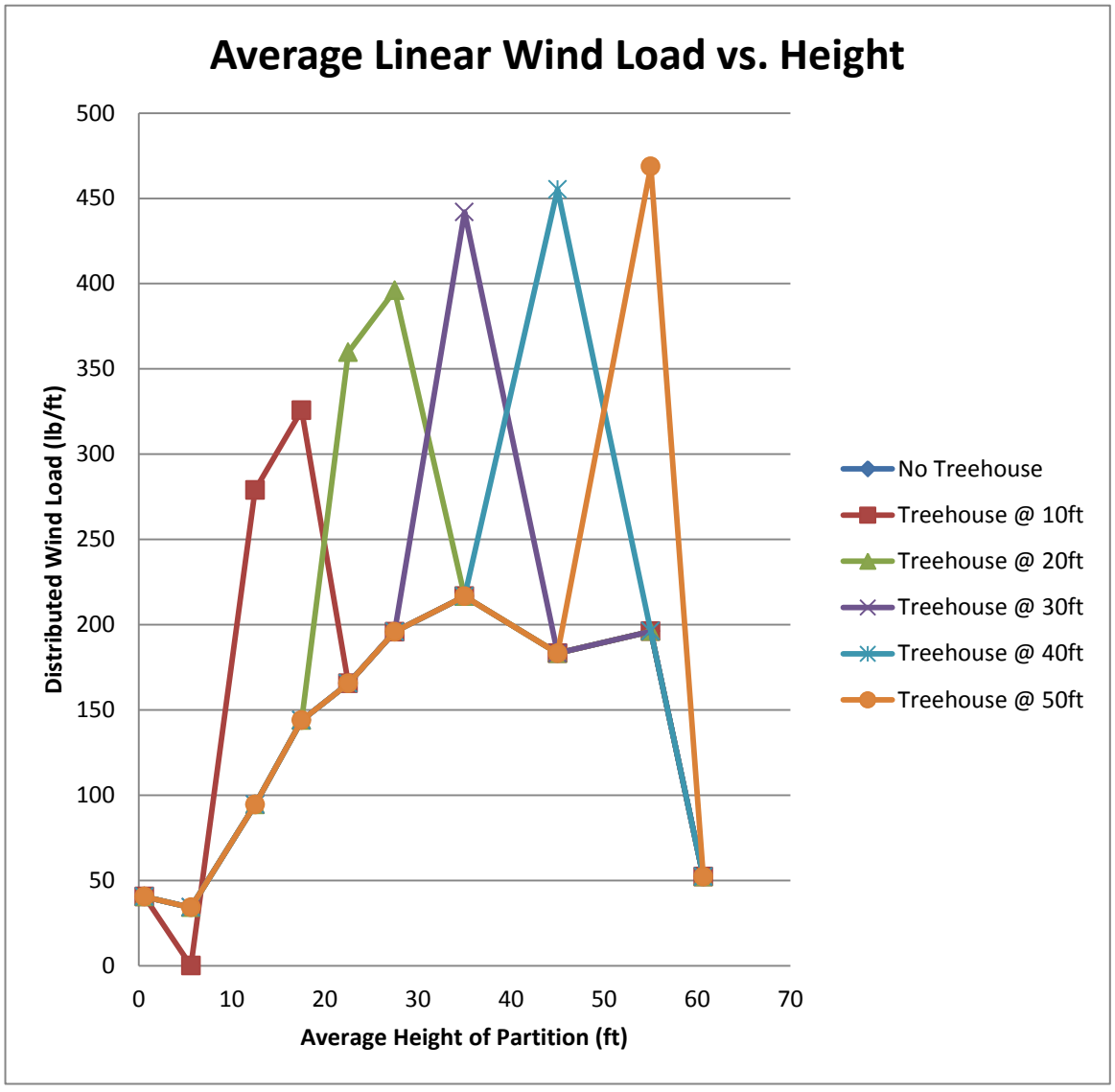

Again, there is a large effect from wind loads at the location of the treehouse. This plot shows spikes in uniformly distributed wind loads at locations where a treehouse

is installed. The peak of each spike increases with the height of the treehouse installation. This is in part due to the exposure factor increasing with height. With these loads, finite element analysis of the tree as a one-dimensional beam was now possible.

4.2 Finite element analysis of a tree-treehouse system under wind loads

The code reproduced in Appendix 4 was run in MATLAB as a finite element analysis for a 1-D beam. The tree above was modeled as a cantilever beam with 12 discrete elements, each with its own constant section properties. There were a total of 39 degrees of freedom. The analysis was run six times in total, with no treehouse, and then with the treehouse at 10, 20, 30, 40, and 50 feet. For each trial, only the uniformly distributed loading was changed along the beam to reflect the change in projected areas with treehouse location.

4.2.1 Elastic analysis principles and tree geometry

To balance the lateral loads, internal moment increases from loading to the cantilevered end support, or the roots in the case of a tree (Leet, Uang, & Gilbert, 2008). For beams in pure flexure, the American Forest & Paper Association (AF & PA) (2006) uses elastic analysis to determine stresses, and tells us that the most critical bending stresses are located at the outermost longitudinal fiber, and are given as:

$$f_b = \frac{Mc}{I} = \frac{M}{S}$$

where f_b is stress due to bending, M is the moment at the location of interest, c is the distance from the centroid to the outermost fiber, I is the moment of inertia of the cross-section, and $S = \frac{I}{c}$ is the section modulus of the beam.

Assuming a circular cross-section, which most practically describes that of a tree, the moment of inertia is given by

$$I = \frac{\pi r^4}{4}$$

where r is the radius of the tree trunk. Assuming a linear decrease in trunk radius within a specified range of heights, the stresses felt along the beam change on the order of $\frac{1}{z^3}$, where z is the height of the tree.

S and M were defined as functions of z for the first 10 feet. Through differential calculus, the location of maximum bending stress was found to be at a distance 1.58 feet above the root flare. This would serve as the fixed end of the beam in the model, with the "stump" considered as a perfectly rigid support. Since bending stresses are most critical at this point, the rigidity of the stump is assumed to have little effect on determining the value of the maximum stress.

Another consideration specific to this tree's geometry was that the tree bifurcated between twenty and twenty-five feet, and then branched out into many sections at a short distance higher. This made calculation of a precise area moment of inertia extremely difficult. Therefore, an area moment of inertia using the parallel axis theorem was approximated for twenty-five feet and the area moment of inertia was set at a value arbitrarily large for points above twenty-five feet. This effectively makes the top of the tree very stiff, but still allows loads to be transferred down the stem. It is assumed to

have little effect on stresses near the base. Below is a sketch of the tree modeled as a finite element beam:

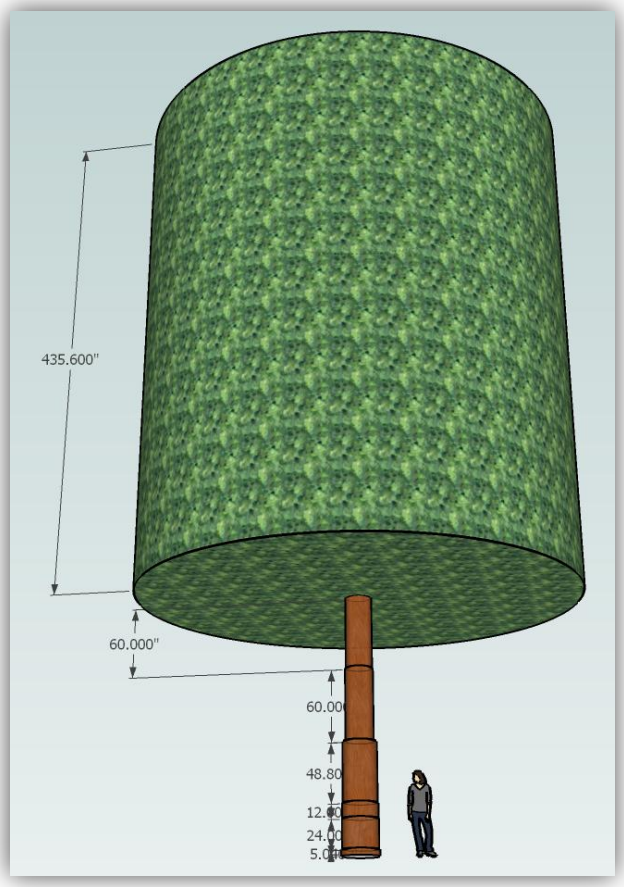

Figure 9. Tree as a finite element beam

The above figure shows the tree modeled as a finite element beam complete with design assumptions. The large section at the top is actually a composite of three ten foot sections and a smaller 1.3 foot section. As described above, the section properties were altered to make the section very stiff. Since gravity loads are not included in analysis, the size of the section only serves to make it stiffer.

4.2.2 The finite element method for a 1-D beam (direct stiffness method)

This method, explained by Reddy (1993), has become a standard method for structural analysis of two-dimensional beams and frames. Leet, Uang, and Gilbert (2008) focus on this method as a means to determine deflections and reactions in indeterminate beams. The method involves discretizing a structure into elements of known structural properties and loadings.

Any uniformly distributed loads are converted into equivalent fixed end forces. In the case of a tree, each element is fixed to the next, in a column. Therefore, the uniformly distributed wind load is calculated as an equivalent set of fixed-end forces for each element. Overlapping fixed-end forces are added together at each end. The result is an equivalent beam with a lateral point load acting at the end of each element.

Next, a 6 × 6 element stiffness matrix, given by:

$$k' = \begin{bmatrix} \frac{4EI}{L} & \frac{2EI}{L} & \frac{6EI}{L^2} & -\frac{6EI}{L^2} & 0 & 0 \\ \frac{2EI}{L} & \frac{4EI}{L} & \frac{6EI}{L^2} & -\frac{6EI}{L^2} & 0 & 0 \\ \frac{6EI}{L^2} & \frac{6EI}{L^2} & \frac{12EI}{L^3} & -\frac{12EI}{L^3} & 0 & 0 \\ -\frac{6EI}{L^2} & -\frac{6EI}{L^2} & -\frac{12EI}{L^3} & \frac{12EI}{L^3} & 0 & 0 \\ 0 & 0 & 0 & 0 & \frac{AE}{L} & -\frac{AE}{L} \\ 0 & 0 & 0 & 0 & -\frac{AE}{L} & \frac{AE}{L} \end{bmatrix}$$

where E is the modulus of elasticity, I is the area moment of inertia, A is the cross-sectional area, and L is the length, is calculated for each element. The local stiffness

matrix is then assembled into a large global stiffness matrix, by adding corresponding elements together. Natural and essential boundary conditions are imposed. In the case of the treehouse, the fixed end of the beam is set to zero deflection. Matrix algebra is then performed for the equation:

$$[K]\{U\} = \{P\}$$

where $[K]$ is the stiffness matrix, $\{U\}$ is the translational and rotational deflections, and $\{P\}$ represents the total known fixed-end forces, point-loads, and reactions for the entire beam. From this, unknown quantities of the vector $\{U\}$ are determined.

The newly discovered deflections are then used in the above equation to find unknown values for $\{P\}$. Of particular value are the reactions, which are employed in elastic analysis to calculate the stresses at the critical location as described below (Leet, Uang, & Gilbert, 2008).

4.2.3 Using the 1-D beam code to calculate stresses and deflections

Based on field data and through approximations of diameter using pixel counts from the silhouetted image, the section properties for elements below twenty-five feet were determined. The area, moment of inertia, modulus of elasticity taken from the Stuttgart table for Black Poplar, length, and uniformly distributed load for each element were set as input for beam.m. Connectivity was specified as a straight beam. The essential boundary conditions were specified as zero at the critical stress location. The analysis was run for each loading scenario, corresponding to treehouse location.

The following results were obtained from running beam.m for these six scenarios:

Table 2. Finite element analysis results

	Treehouse Location (ft)					
	None	**10**	**20**	**30**	**40**	**50**
Max Moment (million lb-in.)	3.750	4.025	4.286	4.629	5.137	5.468
Max Bend. Stress (psi)	1354.	1453.	1547.	1671.	1855.	1975.
Deflection at treehouse mid-ht (ft.)	2.21 @top	0.125	0.5271	1.162	2.009	2.954

Table 2 shows the results of the finite element analysis, which include the max moment, maximum bending stress, and deflection at the mid-height of the treehouse for each treehouse location. The figure below plots the maximum stresses for the tree at its critical location:

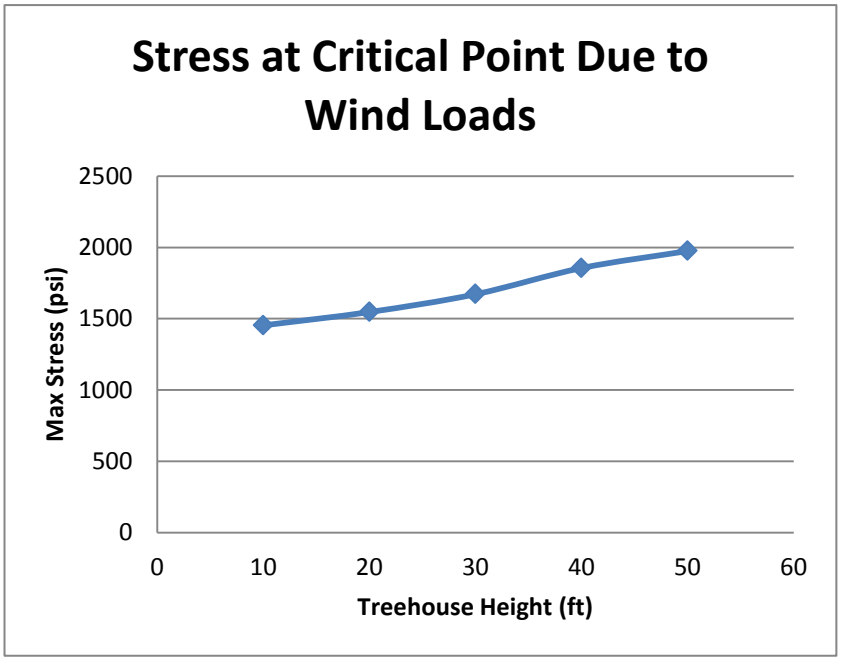

Figure 10. Critical stresses near base of tree due to wind loads

This plot shows how stress at the critical location increases at an approximately linear rate as the placement of the treehouse becomes higher. Compressive strength for this material is estimated to be $2900\ psi$, which is greater than any stresses caused solely by wind loads (Brudi & van Wassenaer, 2001). For this reason, a maximum allowable compressive load was calculated for each treehouse location as well. These data are symmetrical in shape to that in Figure 10, shown in Figure 11 below:

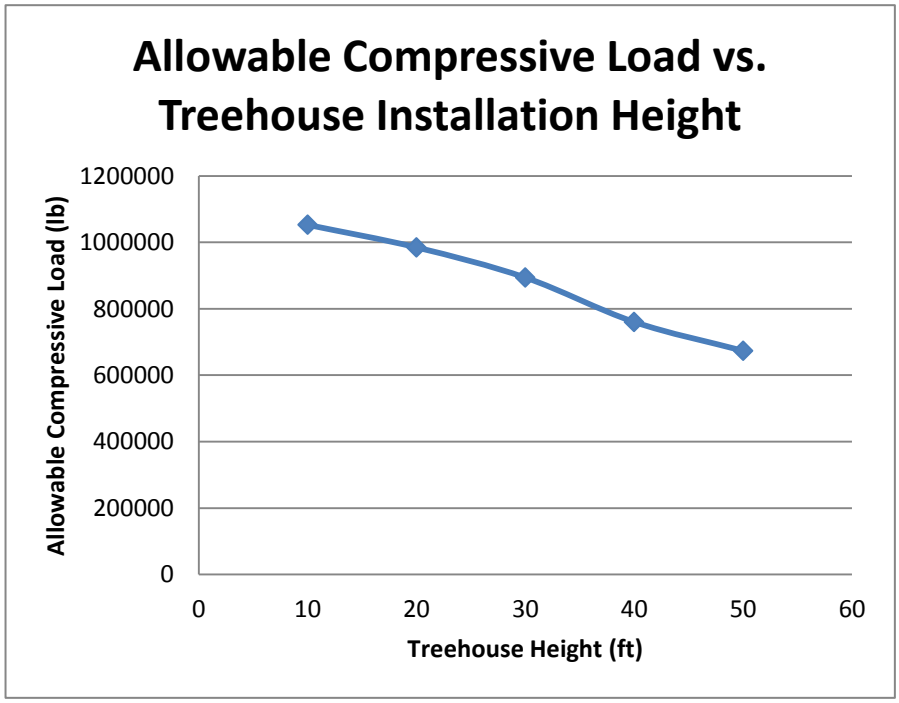

Figure 11. Allowable compressive load vs. treehouse installation height

This figure shows that as placement of a treehouse is chosen to be higher, the tree is unable to carry as much compressive load. Allowable gravity load is approximated by a linear decrease with respect to treehouse location height. These data do not include buckling or second-order effects, which would compound this phenomenon.

Lateral deflections were also calculated at the location of the treehouse for each treehouse height selection. These data are presented in the figure below:

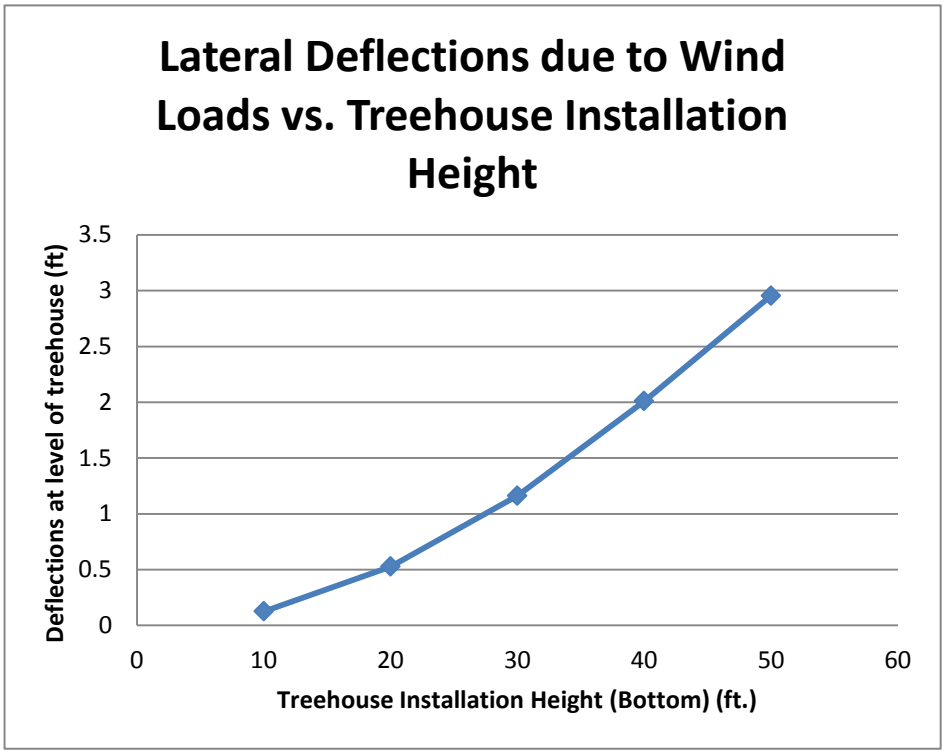

This plot shows how treehouse installation height vastly affects the deflections felt at that height. The effects of treehouse installation height are two-fold: locations further from the ground experience more deflection from geometry, and the higher the treehouse is placed, the greater the uniformly distributed load and the further away from the ground it acts, which causes more bending stress and thus more overall deflection. The trend of increase in deflection at the height of the treehouse is approximately parabolic.

This plot reveals that, at peak wind loads, second-order moment effects would be of great concern, particularly for installations above 15 feet. As deflection increases, the added weight of the treehouse may accentuate this effect.

5. DISCUSSION OF EXISTING CHALLENGES

In addition to the issues raised during the course of this study, several critical issues related to treehouse structures are discussed in this section as a means to direct future work and additional understanding of these novel structures.

5.1 Regulation of treehouse structures

As expounded in the literature review section of this thesis, the challenges of treehouse engineering are numerous. Though this field shares many of the same concerns of traditional structural and foundation engineering, the variables involved can be far more difficult to quantify. In general, the organic structure of trees makes exact analysis exceedingly difficult. In addition, this burgeoning field of engineering lacks the empirical data necessary for accessible design formulas or even qualitative code provisions to be developed. This leads current design practices for public structures to follow a case-by-case procedure, where a unique proposal must be submitted for each project. Since there is no set code to follow, even these design proposals are often qualitative in nature, and their approval may be subjective.

For treehouse structures to become regulated on a larger scale, the field of treehouse engineering must develop as other structural engineering fields have. First of all, the roots and living wood of trees must be considered and studied as legitimate

structural materials with unique abilities to adapt to changes in stress over a long period of time. Through this study, a larger battery of empirical data could be obtained. This data would include living wood strengths and root foundation capacities for a number of different types of mature trees. A history of successful long-term structures and the procedures used to design them could also be useful in this avenue.

Then, as is the case with other types of building materials including steel, concrete, wood, and masonry, an authoritative committee of treehouse engineers must assemble to catalog this information in a publicly available document, which would represent a code for treehouse structures. At a minimum, the document should include accepted qualitative or descriptive design procedures such as those outlined in the literature review. The method for determining wind-induced stresses in treehouse structures illustrated in this thesis could possibly be used in this type of document.

5.2 Material strengths for different types of living wood

One of the difficulties in this project was the lack of available material strengths for living wood. Though the *Stuttgart table of wood strength* provided some key values needed for the analysis in Section 4, such as the modulus of elasticity and compressive strength for the living black poplar tree, there are other failure modes that could have been explored. In particular, it was built into the MATLAB code used in Section 4 to calculate the shear force resultant due to wind loads. Therefore, these values were calculated at a location that may have been in close proximity to the critical location for shear, but served little purpose without an available shear strength value for the living wood type.

It is hypothesized that the relatively heavy self-weight of a mature tree will dominate any tensile stress, such as those caused by wind, and thus deny a tree from failing in tension. However, a more in depth investigation is certainly required. In this thesis, tensile strengths for living wood were not found, but NDS provides these values as a possible failure mode for dry wood. A possible avenue for future research would be to determine the tensile strength of different types of trees, and to then seek a statistically significant ratio of strength between living and dry wood. NDS provides such a ratio between green and dry wood. It is possible that this or a similar ratio could be used.

5.3 The difficulty of geometry in treehouse engineering

Throughout the course of this thesis, the foremost difficulty in treehouse engineering was found to be determining a reasonable approximate geometry of an individual tree. There are far-reaching implications associated with this issue. First of all, without the shape of the tree, the volume, and thus the self-weight cannot be determined. It is assumed that if a volume could be found, average density could then be used to find an approximate weight of the tree. Treehouse structural loads could then be added at the location of installation. This would allow the total dead loads to be determined at locations of critical stress. The effect of this and other loads could then be compared with the strength of living wood as a structural material.

Another disadvantage to not having an approximate shape of the tree is the inability to determine snow, rain and wind loads on the tree itself. Wind loads were investigated in detail in this thesis. Expanding on this analysis, it is hypothesized that finding the projected area of the tree from an overhead point of view would allow an

engineer to calculate a sum of these loads. The same method of silhouettes explicated in this thesis could then be used in a similar way to determine this plan view area, and thus the rain and snow loads. The practical concern of a means to photograph the tree from a sufficient elevation, such as a helicopter, was an obstacle for implementation of the silhouette method in this way. Photography from underneath the tree did not achieve desired results.

An avenue of future research would be to use multiple silhouettes to determinate the volume and generate a three-dimensional wireframe of a tree. Lee, Xu, Eifert, and Zhan (2006) used six silhouettes from different angles to find the volume of much smaller plants. For trees, a perhaps more accurate and practical technology, similar to that used for photogrammetric 3D image capturing, could also be developed and used to create a three-dimensional wireframe of a tree. Many nodes, or markers, could be placed on the tree, and photographed from several angles. This, coupled with three-dimensional finite element based stress analysis software could produce interesting results.

5.4 Buckling and second order effects

Mattheck (1991), in his book Trees: The Mechanical Design, mentions that no tree has ever buckled under its own weight. Despite this statement, it is hypothesized that a tree under the increased loading of a structure may still buckle, especially if the structure is installed high on the tree where limbs have a small cross-sectional area. A particular area of interest could be the study of local buckling at higher altitude installations.

Additionally, because of the large deflections observed in the results of the finite element analysis conducted in this thesis, second-order moment effects should be investigated, especially if dead loads of the tree-treehouse system can be approximated at different locations. These effects might more easily be calculated if a three-dimensional wireframe can be developed.

5.5 Secondary Effects of Rain, Snow, and Ice

It is hypothesized that rain and melting snow affect the strength of living wood. Since trees are exposed to the elements, a direction for future research might be load-bearing branch strength in rainy, snowy, or icy conditions. Empirical data, which compares loading capacity in both dry and wet conditions, could be collected.

6. CONCLUSIONS

This thesis examined stresses induced from wind loads on a single-tree installation of treehouse using the finite element method and a novel method of calculating projected area and wind loads. The 20 foot by 10 foot high treehouse was represented by a rectangle placed along the 61.3 foot cottonwood tree at five different heights: 10, 20, 30, 40, and 50 feet. Silhouetting was used to find the projected area of the tree with the treehouse superimposed at each location. This case study is meant as an initial foray into the much more complex behavior of wind effects on treehouse structures, but is believed to be the first study of its kind.

The key results of this work are as follows:

• Maximum wind loads were found to make up approximately 47 percent of the total compressive strength of the tree with no treehouse. This value was increased to 50.1% for a treehouse at 10ft, 53.3% for a treehouse at 20ft, 57.6% for a treehouse at 30ft, 64.0% for a treehouse at 40ft, and 68.1% for a treehouse at 50ft.

• Bending stress caused by wind loads was estimated to increase linearly with treehouse installation height. In relation to this, the allowable resultant force due to all gravity effects was estimated to decrease linearly.

• Deflections due to wind loads at the location of the treehouse were estimated to increase with treehouse location at a parabolic rate.

There were several other conclusions to this work, but additional data related to the elastic modulus and other basic parameters of the tree would be required before additional conclusions can be drawn. It is hoped that these trends will provide the basis for more detailed investigations of this topic.

7. WORKS CITED

Ambrose, J. (2002). *Simplified Mechanics and Strength of Materials.* New York: John Wiley & Sons.

American Forest & Paper Association, American Wood Council. (2006). *National Design Specification® for Wood Construction (2005 Ed.).* Washington, DC: American Forest & Paper Association, Inc.

Atlas Obscura. (2011). *Le Chêne Chapelle - The Chapel Oak*. Retrieved March 12, 2011, from Atlas Obscura: http://atlasobscura.com/place/chapel-oak

Bodig, J., & Jayne, B. A. (1993). *Mechanics of wood and wood composites (Reprint ed.).* Malabar: Krieger Pub.

Brudi, E., & van Wassenaer, P. (2001). Trees and Statics: Nondestructive Failure Analysis. In E. T. Smiley, & K. D. Coder (Ed.), *Tree Structure and Mechanics Conference Proceedings: How Trees Stand Up and Fall Down* (pp. 53-69). Savannah: The International Society of Aroboriculture.

Das, B. M. (2006). *Principles of Geotechnical Engineering (6th Ed.).* Toronto: Thomson Learning.

Fraedrich, B. R., & Smiley, E. T. (2001). Assessing the Failure Potential of Tree Roots. In E. T. Smiley, & K. D. Coder (Ed.), *Tree Structure and Mechanics Conference Proceedings: How Trees Stand Up and Fall Down* (pp. 159-163). Savannah: The International Society of Aroboriculture.

Fulton, P. (2007). *Build your own treehouse*. Retrieved March 11, 2011, from The Treehouse Guide: http://thetreehouseguide.com/building.htm

Fulton, P. (2010). *Professional tree house building companies*. Retrieved March 12, 2011, from The Treehouse Guide: http://www.thetreehouseguide.com/links-builders.htm

Garnier, M. (n.d.). *Layout*. Retrieved March 12, 2011, from Out'n'About treehouse construction: http://www.treehouses.com/treehouse/construction/layout.html

Garnier, M. (n.d.). *LegaliTrees*. Retrieved March 12, 2011, from Out 'n' About Treesort: http://treehouses.com/treehouse/treesort/legal.html

Garnier, M. (n.d.). *Select tree*. Retrieved March 12, 2011, from Out'n'About treehouse construction: http://www.treehouses.com/treehouse/construction/selectree.html

Garnier, M. (n.d.). *The Garnier Limb*. Retrieved March 12, 2011, from Out 'n' About treehouse construction: http://treehouses.com/treehouse/construction/Garnier%20Limb%20Page.cfm

Gilman, E. F. (2001). Branch-to-Stem Diameter Ratio Affects Strength of Attachment. In E. T. Smiley, & K. D. Coder (Ed.), *Tree Structure and Mechanics*

Conference Proceedings: How Trees Stand Up and Fall Down (pp. 97-98). Savannah: The International Society of Aroboriculture.

Graham, A. W. (2001). A Simple Model for Studying Cable Systems: A Biomechanical Demonstration. In E. T. Smiley, & K. D. Coder (Ed.), *Tree Structure and Mechanics Conference Proceedings: How Trees Stand Up and Fall Down* (pp. 113-123). Savannah: The International Society of Aroboriculture.

Greenwood, C. (2010, February 15). (W. E. Bradley, Interviewer)

Greenwood, C. S. (2005). *Oak Post and Knee Brace with Glue Lam Beams.* Failure Load Evaluation, Greenwood Engineering, Cave Junction.

Greenwood, C. S. (2006). *Universally Accessible Tree House.* Proposal, Mt. Airy Park, Cincinnati.

Greenwood, C. (2007). *Treehouse Engineering - About Trees*. Retrieved March 12, 2011, from Treehouse Engineering: http://www.treehouseengineering.com/abouttrees.html

Greenwood, C. (2007). *Treehouse Engineering - Analysis*. Retrieved March 12, 2011, from TreehouseEngineering.com: http://www.treehouseengineering.com/analysis.html

Greenwood, C. (2007). *Treehouse Engineering - Research*. Retrieved March 12, 2011, from TreehouseEngineering.com: http://www.treehouseengineering.com/research.html

Greenwood, C., & Garnier, M. (n.d.). *Habitable Treehouses: Not as Simple as Swiss Family Robinson.* Retrieved March 12, 2011, from Out'n'About treehouse construction: http://www.treehouses.com/treehouse/construction/engineering.html

Henderson, P., & Mornement, A. (2005). *Treehouses.* London: Frances Lincoln Ltd.

Hochman, D. (2010, March). Back to the trees. *Forbes Life* , pp. 71-73.

Jacobson, A. L. (2001). *How Long Do Trees Live?* Retrieved March 17, 2011, from Arthur Lee Jacobson: http://www.arthurleej.com/a-oldtrees.html

Kane, B. (2001). Comparing Formulas That Assess Strength Loss Due to Decay in Trees. In E. T. Smiley, & K. D. Coder (Ed.), *Tree Structure and Mechanics Conference Proceedings: How Trees Stand Up and Fall Down* (pp. 71-87). Savannah: The International Society of Aroboriculture.

Lee, D. J., Xu, X., Eifert, J., & Zhan, P. (2006). Area and volume measurements of objects with irregular shapes using multiple silhouettes. *Optical Engineering , 45* (2), 027202-1 - 027202-11.

Leet, K. M., Uang, C.-M., & Gilbert, A. M. (2008). *Fundamentals of Structural Analysis (3rd ed.).* New York: McGraw-Hill.

Luley, C. J., Pleninger, A., & Sisinni, S. (2001). The Effect of Wind Gusts on Branch Failures in the City of Rochester, New York, U.S. In E. T. Smiley, & K. D. Coder

(Ed.), *Tree Structure and Mechanics Conference Proceedings: How Trees Stand Up and Fall Down* (pp. 103-109). Savannah: The International Society of Aroboriculture.

Mattheck, C. (1991). *Trees: The Mechanical Design.* Berlin: Springer-Verlag.

Mattheck, C., Betge, K., & West, P. (1994). Breakage of hollow tree stems. *Trees , 9*, 47-50.

Mattheck, C., Bethge, K., & Schafer, J. (1993). Safety Factor in Trees. *Journal of Theoretical Biology , 165*, 185-189.

Milton, J. (2008, April 18). *How to Measure the Height of a Tree.* Retrieved March 20, 2011, from Tree News: http://jessemilton.blogspot.com/2008/04/how-to-measure-height-of-tree.html

Moore, J. R., & Maguire, D. A. (2001). The Mechanics of Trees Under Wind Loading. In E. T. Smiley, & K. D. Coder (Ed.), *Tree Structure and Mechanics Conference Proceedings: How Trees Stand Up and Fall Down* (pp. 39-49). Savannah: The International Society of Aroboriculture.

Nelson, P. (2004). *Treehouses of the World.* New York: harry n. abrams, inc.

Nelson, P., & Hadden, G. (1997). *Home Tree Home: Principles of Treehouse Construction and Other Tall Tales.* New York: Penguin Books.

Niklas, K. J. (2001). Wind, Size, and Tree Safety. In E. T. Smiley, & K. D. Coder (Ed.), *Tree Structure and Mechanics Conference Proceedings: How Trees Stand Up and Fall Down* (pp. 3-19). Savannah: The International Society of Aroboriculture.

Peltola, H., Kellomaki, S., Hassinen, Hassinen, A., & Granander, M. (2000). Mechanical stability of Scots pine, Norway spruce and birch: an analysis of tree-pulling experiments in Finland. *Forest Ecology and Management , 135*, 143-153.

Reddy, J. N. (1993). *An introduction to the finite element method.* New York: McGraw-Hill.

Stokes, A., Fourcaud, T., & Berthier, S. (2001). Tree Resistance to Wind, or Strange Things That Happen Under Stress. In E. T. Smiley, & K. D. Coder (Ed.), *Tree Structure and Mechanics Conference Proceedings: How Trees Stand Up and Fall Down* (pp. 21-36). Savannah: The International Society of Aroboriculture.

Wenning, A. (2009). *Treehouses: Construction and Design Manual.* Berlin: DOM publishers.

Wilson, B. F., & Archer, R. R. (1979). Tree Design: Some Biological Solutions to Mechanical Problems. *BioScience , 29* (5), 293-298.

APPENDIX 1: STUTTGART TABLE OF WOOD STRENGTH (PARTIALLY REPRODUCED FROM (BRUDI & VAN WASSENAER, 2001)

Species (Latin Name)	Common Name	E $\left(\frac{N}{mm^2}\right)$	E (psi)	Long. Strength	Long. Strength (psi)	Elastic Limit (%)	Aerodynamic Drag (cw)
Liriodendron tulipifera	American tulip tree	5000	7.25E+05	17	2.47E+03	0.34	0.25
Alnus glutinosa	Black Alder (Birch)	8000	1.16E+06	20	2.90E+03	0.25	0.25
Robinia pseudoacacia	Black Locust	7050	1.02E+06	20	2.90E+03	0.28	0.15
Acer negundo	Box Elder, Maple Ash	5600	8.12E+05	20	2.90E+03	0.36	0.25
Poplus nigra	Black Poplar (Cottonwood)	6520	1.00E+06	20	2.90E+03	0.31	0.2
Fraxinus excelsior	Common Ash	6250	9.06E+05	26	3.77E+03	0.42	0.20
Cedrus deodora	Deodar Cedar	7650	1.11E+06	15	2.18E+03	0.2	0.20
Quercus robur	English oak	6900	1.00E+06	28	4.06E+03	0.41	0.25
Fagus sylvatica	European Beech	8500	1.23E+06	22.5	3.26E+03	0.26	0.28
Larix decidua	European Larch	5035	7.30E+05	17	2.47E+03	0.32	0.15
Abies alba	European Silver Fir	9500	1.38E+06	15	2.18E+03	0.16	0.20
Acer campestre	Field Maple	6000	8.70E+05	25.5	3.70E+03	0.43	0.25
Sequoiadendron gigantum	Giant Sequoia	4550	6.60E+05	18	2.61E+03	0.4	0.20
Salix alba 'Tristis'	Golden Weeping Willow	7000	1.02E+06	16	2.32E+03	0.23	0.20
Tilia platyphyllos	Large-leafed Linden	8000	1.16E+06	20	2.90E+03	0.25	0.25
Chamaecyparis lawsoniana	Lawson's Cypress	7350	1.07E+06	20	2.90E+03	0.27	0.20
Pinus pinaster	Maritime pine	8500	1.23E+06	18	2.61E+03	0.21	0.20
Quercus rubra	Northern red oak	7200	1.04E+06	20	2.90E+03	0.28	0.25
Picea abies	Norway Spruce	9000	1.31E+06	21	3.05E+03	0.23	0.20
Ulmus glabra	Scots Elm	5700	8.27E+05	20	2.90E+03	0.35	0.25
Pinus sylvestris	Scots pine	5800	8.41E+05	17	2.47E+03	0.29	0.15

Picea omorika	Serbian Spruce	9000	1.31E+06	16	2.32E+03	0.18	0.20
Betula pendula	Silver Birch	7050	1.02E+06	22	3.19E+03	0.31	0.12
Tilia tomentosa	Silver Linden	8350	1.21E+06	20	2.90E+03	0.24	0.28
Acer saccharinum	Silver Maple	6000	8.70E+05	20	2.90E+03	0.33	0.25
Tilia cordata	Small-leaved Linden	8300	1.20E+06	20	2.90E+03	0.24	0.25
Acer saccharum	Sugar Maple	5450	7.90E+05	20	2.90E+03	0.37	0.25
Castanea sativa	Sweet Chestnut	6000	8.70E+05	25	3.63E+03	0.42	0.25
Acer pseudoplatanus	Sycamore Maple	8500	1.23E+06	25	3.63E+03	0.29	0.25
Salix alba	White Willow	7750	1.12E+06	16	2.32E+03	0.21	0.20

APPENDIX 2: RESULTS OF TREE CIRCUMFERENCE VS. HEIGHT

Height (ft.)	Tree 1	2	3	4	5	6
0	51	97	108.5	121	120	121
2	46	90.5	90	109	107	106
4	46	89	84.5	102.5	100	96.5
5	46	86	82	104	97.5	95.25
6	46	83	79.5		95	94

Table A2. 1: Circumferences of Six Trees at Different Heights

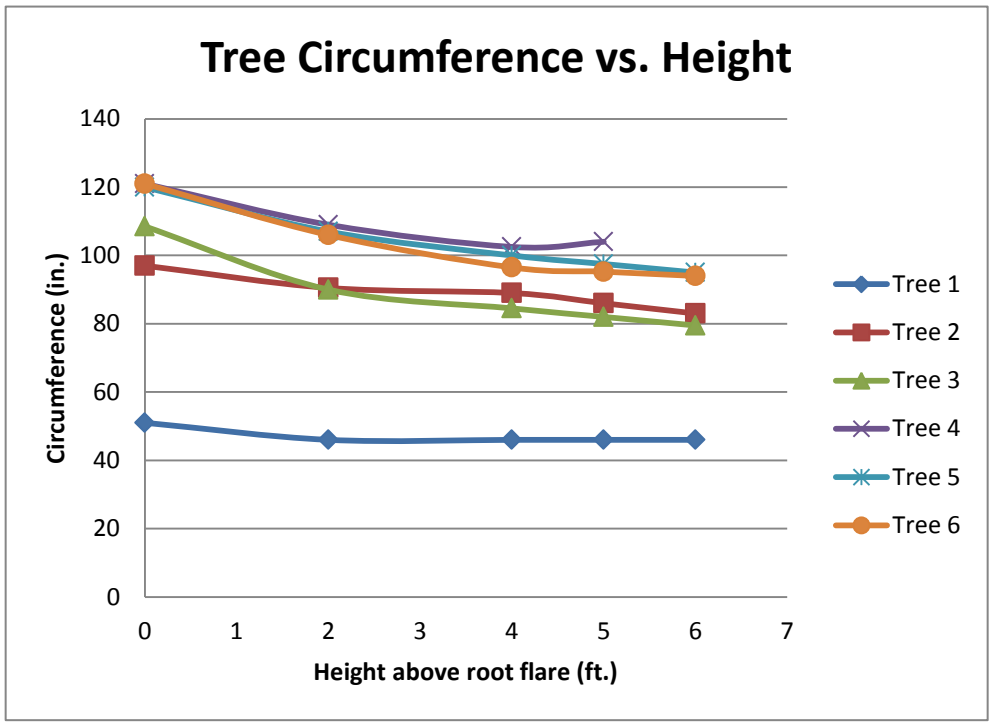

Figure 12. Tree circumference vs. height for six trees

APPENDIX 3: PROJECTED AREA OF A PRISTINE (BINARY) TREE SILHOUETTE

This section helps to detail the process of determining the projected area of a tree from a silhouette that is used in Section 4.1.

In the analysis below, a binary silhouette photograph from Google image search was used:

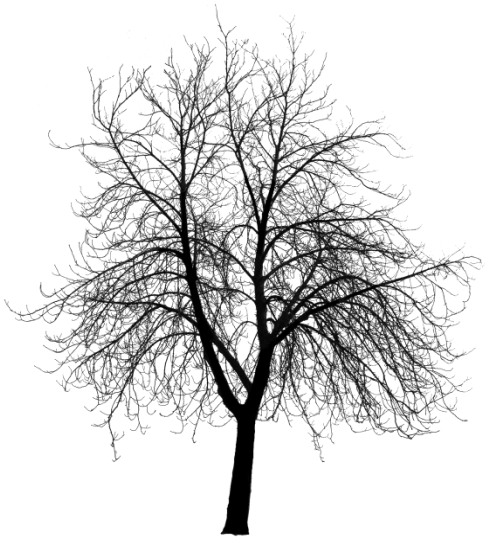

Figure 13. Binary silhouette of a tree

The binary nature of this photograph allows human error associated with photography to be minimized. As a first step, the photo was partitioned into five

sections, the heights (in pixels) 201-600, 601-1000, 1001-1400, 1401-1800, and 1801-2200. Below are photos of the first two sections:

Figure 14. Binary silhouette, 201-600 pxl

Figure 15. Binary silhouette, 601-1000 pxl

The pattern continues for each range of pixels. Once the image was partitioned, the areas could be calculated for each range of pixels, which can then be equated to the actual tree height ranges, if known. To calculate the area of the silhouette of each partition, the software package ImageJ was employed.

This software was used to count the number of black pixels for the photo. To do this, each photo was transformed to a RBG image type, and color threshold selection tool was used. With this tool, only the dark pixels of the silhouette are selected. Once these pixels are chosen as the set to analyze, the Measure tool was utilized to count the number

of dark pixels. This produces the area in pixels of the silhouette for the specified height range of the photo. The results for each silhouette are tabulated below:

Table 3. ImageJ Results for Five Pixel Height Ranges

Height (pxl)	Area (pxl^2)
400	80924
800	273039
1200	161392
1600	72663
2000	2639

The heights 400, 800, 1200 represent the mean pixel height of each 400 pixel section of the silhouette. For example, a height of 400 pixels implies that the section of the silhouette that was measured was from 200 to 600 pixels. These results give the following distribution of the area versus average height:

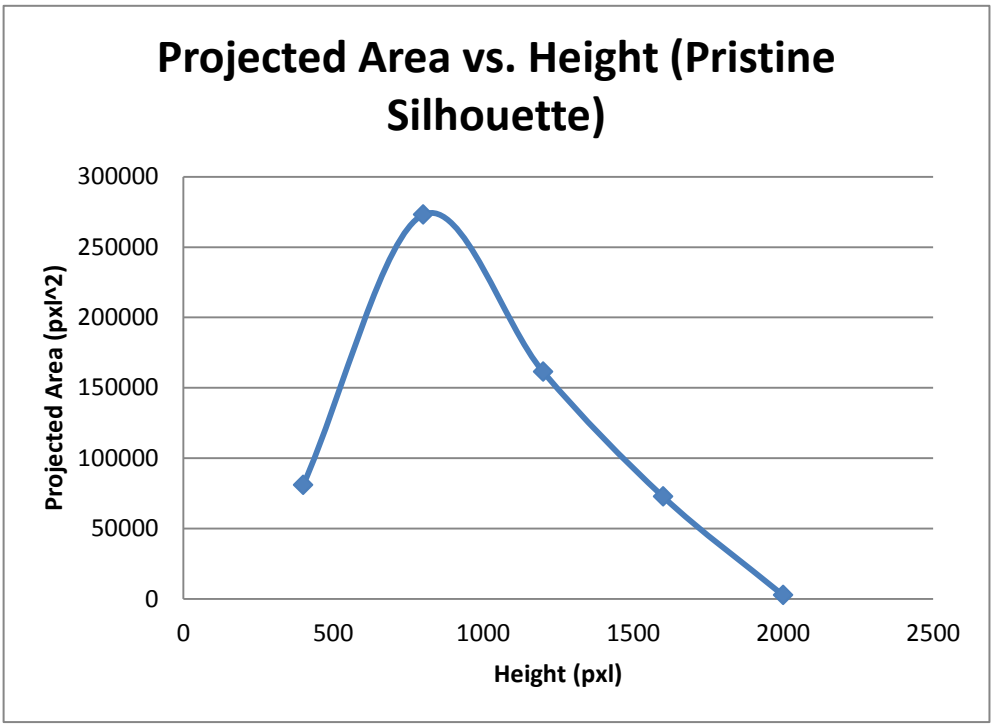

Figure 16. Projected area vs. height of a pristine silhouette

With a known scaling factor, these results can be converted from square pixels to square feet, as is done in Section 4.1 above.

APPENDIX 4. BEAM.M (MATLAB CODE)

```
% Will Bradley
% CIVE 566
% Beam FE
% Variables used:
% nelements = number of elements
% ndof = number of degrees of freedom
% nebc = number of essential boundary conditions (disp or rot)
% nnbc = number of natural boundary conditions (force or moment)
% A(i) = area of cross-section of element i
% E(i) = MOE of element i
% I(i) = MOI of element i
% L(i) = length of element i
% theta(i) = angle from horizontal of element i
% currel = the number of the current element
% Klocal(6,6,k) = 6x6 Stiffness matrix of element k in local coordinates
% Kglobal = 6x6 Global stiffness matrix of current element
% Kstructure = nxn Global structure stiffness matrix
% Kbar = nxn Global structure stiffness matrix with boundary conditions
% Ulocal(6,i) = 6x1 local displacement vector for element i
% Ubar = nx1 displacements after B.C.'s
% Ustructure = Displacements for entire frame
% Pstructure = Forces and moments for entire frame
% Plocal(6,i) = 6x1 local Force/Moment vector for element i
% Pbar = nx1 Structure Forces and moments vector from B.C.'s
% idarray(n,i) = connectivity array for current element i
% Pfelocal(6,j) = 6xn local fixed end forces for element j
% Pfeglobal = 6x1 global fixed end forces for current element
% Pfestructure = fixed end forces for entire structure
% Gamma(6,6,i) = a 6x6 local-to-global rotation matrix for element i
% ebcloc(i) = location of known displacement or rotation
% ebcval(i) = value of known disp or rot corresponding to i of ebcloc
% nbcloc(i) = location of known force or moment
% nbcval(i) = value of known force or moment corresponding to i of nbcloc

clear
load beamdatain -ASCII
%
% Assign input to variables
%
nelements = beamdatain(1,1);
ndof = beamdatain(1,2);
nebc = beamdatain(1,3);
nnbc = beamdatain(1,4);
```

```
%
% Assign beam properties and initialize matrices
%
for currel=1:nelements
   A(currel)=beamdatain(currel+1,1);
   E(currel)=beamdatain(currel+1,2);
   I(currel)=beamdatain(currel+1,3);
   L(currel)=beamdatain(currel+1,4);
   theta(currel)=beamdatain(currel+1,5);
   w(currel)=beamdatain(currel+1,6);
end
for i=1:ndof
   Ustructure(i,1)=0.0;
   Ubar(i,1)=0.0;
   Pstructure(i,1)=0.0;
   Pbar(i,1)=0.0;
   Pfestructure(i,1)=0.0;
end
Ulocal=zeros(6,1);
Klocal=zeros(6,6,nelements);
Kglobal=zeros(6);
Kstructure=zeros(ndof);
Kbar=zeros(ndof);
Pfelocal=zeros(6,nelements);
idarray=zeros(6,nelements);
Gamma=zeros(6,6,nelements);
Plocal=zeros(6,nelements);
Pfelocal=zeros(6,nelements);
%
% Loop over whole structure:
% Get Gamma, Klocal and fixed-end forces for each element.
%
for currel=1:nelements
   Gamma(3,3,currel)=1;
   Gamma(6,6,currel)=1;
   Gamma(1,1,currel)=cosd(theta(currel));
   Gamma(1,2,currel)=sind(theta(currel));
   Gamma(2,1,currel)=-sind(theta(currel));
   Gamma(2,2,currel)=cosd(theta(currel));
   Gamma(4,4,currel)=Gamma(1,1,currel);
   Gamma(4,5,currel)=Gamma(1,2,currel);
   Gamma(5,4,currel)=Gamma(2,1,currel);
   Gamma(5,5,currel)=Gamma(2,2,currel);
   Klocal(1,1,currel)=A(currel)*E(currel)/L(currel);
   Klocal(1,4,currel)=-A(currel)*E(currel)/L(currel);
   Klocal(2,2,currel)=12*E(currel)*I(currel)/L(currel)^3;
   Klocal(2,3,currel)=6*E(currel)*I(currel)/L(currel)^2;
   Klocal(2,5,currel)=-12*E(currel)*I(currel)/L(currel)^3;
   Klocal(2,6,currel)=6*E(currel)*I(currel)/L(currel)^2;
   Klocal(3,3,currel)=4*E(currel)*I(currel)/L(currel);
   Klocal(3,5,currel)=-6*E(currel)*I(currel)/L(currel)^2;
   Klocal(3,6,currel)=2*E(currel)*I(currel)/L(currel);
   Klocal(4,4,currel)=A(currel)*E(currel)/L(currel);
   Klocal(5,5,currel)=12*E(currel)*I(currel)/L(currel)^3;
```

```
   Klocal(5,6,currel)=-6*E(currel)*I(currel)/L(currel)^2;
   Klocal(6,6,currel)=4*E(currel)*I(currel)/L(currel);
   Klocal(3,2,currel)=Klocal(2,3,currel);
   Klocal(4,1,currel)=Klocal(1,4,currel);
   Klocal(5,2,currel)=Klocal(2,5,currel);
   Klocal(6,2,currel)=Klocal(2,6,currel);
   Klocal(5,3,currel)=Klocal(3,5,currel);
   Klocal(6,3,currel)=Klocal(3,6,currel);
   Klocal(6,5,currel)=Klocal(5,6,currel);
   Kglobal=transpose(Gamma(1:6,1:6,currel))*Klocal(1:6,1:6,currel)*Gamma(1:6,1:6,currel);
   Pfelocal(1,currel)=0;
   Pfelocal(2,currel)=w(currel)*L(currel)/2;
   Pfelocal(3,currel)=w(currel)*L(currel)^2/12;
   Pfelocal(4,currel)=0;
   Pfelocal(5,currel)=w(currel)*L(currel)/2;
   Pfelocal(6,currel)=-w(currel)*L(currel)^2/12;
   Pfeglobal=transpose(Gamma(1:6,1:6,currel))*Pfelocal(:,currel);
%
% Read in connectivity for current element
%
   for i=1:6
      idarray(i,currel)=beamdatain(currel+nelements+1,i);
   end
%
% Assemble global values in Kstructure and Pfestructure for current element
%
   for i=1:6
      Pfestructure(idarray(i,currel),1)=Pfeglobal(i,1)+Pfestructure(idarray(i,currel,1));
      for j=1:6

Kstructure(idarray(i,currel),idarray(j,currel))=Kglobal(i,j)+Kstructure(idarray(i,currel),idarray(j,currel));
      end
   end
end
%
% Kstructure and Pfestucture are assembled.  Apply Boundary Conditions.
% First make copy of Kstructure matrix for application of B.C.'s
%
Kbar = Kstructure;
%
% Assign ebc and nbc locations and values from data
%
for i=1:nebc
   ebcloc(i)=beamdatain(1+2*nelements+i,1);
   ebcval(i)=beamdatain(1+2*nelements+i,2);
end
for i=1:nnbc
   nbcloc(i)=beamdatain(1+2*nelements+nebc+i,1);
   nbcval(i)=beamdatain(1+2*nelements+nebc+i,2);
end
%
% Zero out each row and column of known disp/rot.  Put a 1 in the diagonal.
%
for i=1:nebc
```

```
   Kbar(:,ebcloc(i))=0.0; %sets row = 0
   Kbar(ebcloc(i),:)=0.0; %sets column = 0
   Kbar(ebcloc(i),ebcloc(i))=1; %sets diagonal = 1
end
%
% All Pbar values were initialized to 0 above.
% Now set Pbar values equal to nbcvals at their location.
%
for i=1:nnbc
   Pbar(nbcloc(i),1)=nbcval(i);
end
%
% Include fixed end forces
%
Pbar=Pbar-Pfestructure;
%
% Solve for the unknown displacements, and move all known U's to Ustructure
%
Ubar=Kbar\Pbar;
Ustructure=Ubar;
for i=1:nebc
   Ustructure(ebcloc(i),1)=ebcval(i);
end
%
% Get reactions
%
Pstructure=Kstructure*Ustructure+Pfestructure;
%
% Calculate forces and moment for each element
%
for currel=1:nelements
   Ulocal(:,1)=0; %Zero out Ulocal
   for i=1:6
      for j=1:6
         Ulocal(i,1)=Gamma(i,j,currel)*Ustructure(idarray(j,currel),1)+Ulocal(i,1);
      end
   end
   Plocal(:,currel)=Klocal(:,:,currel)*Ulocal+Pfelocal(:,currel);
end
```